Research Square

Preprints are preliminary reports that have not undergone peer review.
They should not be considered conclusive, used to inform clinical practice,
or referenced by the media as validated information.

Development of engineered ferredoxin reductase systems for the efficient hydroxylation of steroidal substrates

Zhangliang Zhu
Tianjin University of Science and Technology
Xin Gao
Tianjin University of Science and Technology
Zhan Song
Tianjin University of Science and Technology
Chao Li
Tianjin University of Science and Technology
Fuping Lu (fupinglu2016@sina.com)
Tianjin University of Science and Technology
Masaru Tanokura (zlzhu@vip.163.com)
Tianjin University of Science and Technology
Hui-Min Qin (huiminqin@tust.edu.cn)
Tianjin University of Science and Technology

Research

Keywords: 3-ketosteroid-9-hydroxylase; reductase; electron transfer system; 9α-hydroxy-4-androstene-3,17-dione; ferredoxin; whole-cell bioconversion

Posted Date: June 9th, 2020

DOI: https://doi.org/10.21203/rs.3.rs-32899/v1

License: This work is licensed under a Creative Commons Attribution 4.0 International License.
Read Full License

Version of Record: A version of this preprint was published at ACS Sustainable Chemistry & Engineering on October 28th, 2020. See the published version at https://doi.org/10.1021/acssuschemeng.0c07042.

Abstract

Background

9α-hydroxy-4-androstene-3,17-dione (9OHAD), catalyzed by 3-ketosteroid-9-hydroxylase (KSH) using 4-androstene-3,17-dione (AD) as a substrate, is an important precursor for the synthesis of adrenocortical hormones. Whole-cell catalyst in microorganisms with this KSH system for desirable hydroxylated steroids in high purity and productivity have rarely been successful.

Results

The rate-limiting step for the biosynthesis of 9OHAD is catalyzed by the reductase KshB, which is an important component of electrons donor. A sufficient supply system of the cofactor NADH was constructed on KshB by introducing the formate dehydrogenase (FDH) gene. Several reductases were then screened to find a TDO reductase containing a ferredoxin, which showed a maximal NADH activity with a catalytic efficiency (k_{cat}/K_m) of 0.43 s^{-1} μM^{-1} and 54.8% of 9OHAD yield via multienzyme cascade catalysis *in vitro*. TDO mutagenesis was further performed via a protein engineering strategy, resulting in a 2.25-fold improvement in activity and a 74.8% 9OHAD yield. The modification of a Rieske [2Fe-2S] cluster in KshB and TDO showed 9OHAD yields of 56.1% and 74.5% higher than wild-type ones, which implied Rieske [2Fe-2S] ferredoxin strengthening for electrons transferring. The biosynthesis of 9OHAD was further optimized in a whole-cell catalysis system with FDH, KshA, and TDO_M9 mutant with the Rieske [2Fe-2S] ferredoxin (BLKA-RMT-F), resulting in a final production of 5.24 g/L 9OHAD, a considerable yield of 99.3% of theoretical without by-products.

Conclusion

An efficient whole-cell catalyst was constructed with considerable production and yield by modification of a Rieske [2Fe-2S] cluster in TDO with increased the efficiency of electron transfer. This research provided comprehensive insight into the electron transfer system for these steroid hydroxylation reactions and NADH regeneration systems.

Background

Steroid medicines, a vital class of the pharmaceuticals, play an important role in healthy development, life quality, and aging, and they are the second largest category of proscribed medications following antibiotics [1]. There are many clinical applications of steroid medicines, including as anti-tumour, anti-viral, anti-fungal, anti-microbial, and anti-allergy agents [2]. Hydroxylated steroids are pharmaceutically very interesting bioactive compounds. Among them, 9α-hydroxy-4-androstene-3,17-dione (9OHAD), which can be transformed from 4-androstene-3,17-dione (AD) by 3-ketosteroid 9α-hydroxylase (KSH), is an important precursor for synthesizing glucocorticoid drugs by replacing a halogen in the C9α-position [3].

KSH is a two-component class IA type monooxygenase involved in microbial steroid catabolism and is encoded by a Rieske oxygenase (KshA) and a ferredoxin reductase (KshB) [4–6]. KshA contains a Rieske [2Fe-2S] cluster and mononuclear ferrous iron, while KshB also contains [2Fe-2S] cluster, and it requires nicotinamide adenine dinucleotide (NADH) and flavin adenine dinucleotide (FAD) as the electron donors and transfer [5]. KSH enzyme systems for the production of 9α-hydroxylated steroids have been identified in *Rhodococcus erythropolis* SQ1 [7], *R. rhodochrous* DSM43269 [4], and *Mycobacterium tuberculosis* H37Rv [5], and they are important in the cleavage of steroid nucleus in microorganisms, whereas AD and ADD can be stably accumulated by genetic inactivation of KSH in *M. tuberculosis* [8, 9]. The biochemical characterization of KSH has been investigated by heterologous expression in *Escherichia coli* [7, 8, 10]. The activity of KshA, unfortunately, is almost entirely lost after purification due to its instability. However, co-expression of KshA and KshB in *E. coli* can enhance the stability of KshA and increase the hydroxylation activity of KSH, which demonstrates a protein-protein interaction between them [4, 8]. The deletion of the Rieske oxygenase gene in *R. erythropolis* SQ1 abolished the ability to grow on the AD and ADD, indicating that these two components were essential [7]. There have been some reports of the production of 9OHAD produced from AD by heterologous co-expression of the two components in *E. coli* cells with a greater than 60% molar yield of 9OHAD [4]. Yao *et al*. demonstrated a stable accumulation of 9-OHAD in a strain with a 7.33 g/L production from phytosterols by multiple deletions of three KstD genes and overexpression of the KshA gene in the *M. neoaurum* ATCC 25795 strain [11]. Gao *et al*. reported that the 9OHAD production and space-time yield could reach 36.4 g/L and 9.1 g/(L·d) with resting cells of *M. neoaurum* NwIB-yV in a 5-L bioreactor, respectively [12].

In the hydroxylation of steroids, the electrons transferred from NAD(P)H by a ferredoxin reductase are required. The KshB in a KSH system is responsible for donating electrons from NADH and transferring them to KshA via a [2Fe-2S] cluster domain [5]. The cofactor NAD(P)H is essential due to its high cost for application in chemical and pharmaceutical industries [13], and the bioconversion should not occur when NADH is consumed up *in vitro* [14]. Therefore, the NAD(P)H regeneration systems should be established as more economical processes in preparative biotransformation. The enzymatic regeneration mode of NAD(P)H has been widely developed using alcohol dehydrogenases, hydroxy acid dehydrogenases, and several other dehydrogenases [15], of which formate dehydrogenase (FDH) and glucose dehydrogenase (GDH) are commonly used. NAD-dependent FDH is a gold standard enzyme widely used for NADH regeneration at industrial scale only using the low-cost substrate formate, while GDH produces some by-products, such as gluconic acid, lactic acid, and acetic acid [16]. Jaroensuk *et al.* utilized FDH from *Xanthobacter* sp. 91 to regenerate NADH to increase alkanes from fatty acids to about 50% of theoretical yield [17]. Samuel *et al.* achieved the production of 2,3-butanediol from acetoin at 9.3 g/(L·h) with FDH as an NADH regeneration system in *Bacillus subtilis* 168 [18]. Therefore, the use of FDH is an effective strategy for NADH regeneration to improve productivity.

Although detailed information has been obtained about KSH in some microorganisms, attempts to modify this KSH system for desirable sterol substrates in high purity and productivity have rarely been successful. In this study, we focused on the screening and engineering of reductases, including an NADH regeneration system utilizing FDH from *Candida boidinii*, and the reconstruction of iron-sulfur clusters to

strengthen electron transfer. The reductase TDO, containing an additional Rieske [2Fe-2S] ferredoxin, increased the efficiency of electron transfer than that of the original KshB and other reductases. Furthermore, TDO was modified by error-prone PCR for the improvement of NADH activity. Using an electron transfer chain by reductase, combined with an NADH regeneration system, we aimed to establish and optimize an economical and sustainable whole-cell biocatalyst for the efficient bioconversion of 9OHAD from AD. The designed electron transport chain combined with an NADH regeneration with a remarkably higher efficiency of electron transfer has the potential for the production of steroidal substrates in biotransformation processes to improve yields at an industrial scale.

Results And Discussion

Determining the rate-limiting step in producing 9OHAD with KSH

KSH is a two-component Rieske oxygenase (KshAB). The reaction cycle requires two reducing equivalents [5], which originate from NADH, and the resulting electrons are transferred from KshB to KshA (Fig. 1). Over the course of the steroidal transformation, reductases play a crucial role in the electron conversion using NAD(P)H [3]. KSH activities should, therefore, be abolished in the absence of the reductase KshB, which implies that KshB might affect the productivity of 9OHAD in this KSH system [4, 8]. Therefore, the rate-limiting step in producing 9OHAD was investigated using purified KshA and KshB. In the full pathway of this KSH reaction system, a 31.9% yield of 9OHAD was obtained. When only a 20% concentration of KshA enzyme was used in this reaction system, only a subtle effect on the yield of 9OHAD was observed (Fig. 2A). However, when the concentration of KshB was decreased to 20%, a yield of only 14.5% 9OHAD was obtained, meaning a significant decrease of 55% compared with the standard full pathway reaction system. We further investigated the effect of the KshB concentration (10-100%) on this reaction system. The yields of 9OHAD decreased from 31.9% to 5.5% when the concentration of KshB decreased from 100 to 10% (Fig. 2B), which demonstrated that the reductase KshB was a potential rate-limiting enzyme in the hydroxylation reaction for producing 9OHAD.

Construction of an NADH regeneration system

KshB requires the cofactor NADH as an electron donor (Fig. 1) [5]. KSH showed no hydroxylation activity toward AD without the NADH in a reaction mixture [4]. NADH regeneration often results in a significant improvement of whole-cell conversion [19]. The addition of the FDH enzyme was crucial to lower the industrial cost by recycling NADH efficiently in this reaction system. Therefore, the consumption of NADH was determined in this reaction system. The concentrations of NADH were observed to drop significantly from 500 μM and maintained at a low level of 40.3 μM after reaction for 20 min. A fed-batch mode with the addition of NADH, unfortunately, did not work continuously in this reaction system (Fig. 3A). Furthermore, NADH often takes over a considerable proportion of the production cost of steroidal medicines [20]. Therefore, the reconstruction of an NADH regeneration system was required, steady-state kinetic analysis of selected FDH toward NAD^+ was carried out, and the resulting K_m and k_{cat} were 32.02 μM and k_{cat}/K_m 0.34 s^{-1} μM^{-1}, respectively (Fig. S1). FDH and sodium formate were thus added to this

multienzyme cascade catalysis *in vitro* to regenerate NADH as an electron donor (Fig. 1). The rate-limiting step was also investigated via decreasing FDH to 10% (0.025 μM) (Fig. 3B). The concentrations of NADH were increased gradually and reached the same level as that of the original reaction conditions. This indicated that FDH would not affect this NADH regeneration system. Therefore, we used 0.025 μM FDH in the following multienzyme cascade catalysis.

Screening reductases to improve the conversion of AD

As KshB was the rate-limiting step in producing 9OHAD, therefore, we screened the optical ferredoxin reductases by determining activity toward NADH to improve the efficiency of electron transfer in our reaction system. We further screened the reductase genes of KshB, DMR1, DMR2, DMR3, and TDO, which all have potential for the hydroxylation reaction of AD. The kinetic parameters of these reductases were determined with NADH as a substrate (Table 2 and Fig. S2). The affinity (K_m) values were between 55.72 and 182.1 μM, and the catalytic efficiencies (k_{cat}/K_m) were between 0.11 and 0.43 s^{-1} μM^{-1}, respectively. The reductase of TDO showed a higher activity than other reductases, with K_m of 65.37 μM and k_{cat}/K_m of 0.43 s^{-1} μM^{-1}. TDO contains the reductase TDO-R and the Rieske [2Fe-2S] cluster TDO-F [21]. Therefore, the combination of TDO-R and TDO-F may improve the efficiency of electrons transfer for our catalysis scheme. The yield of 9OHAD reached 54.8% using TDO as a reductase compared with that by KshB (42%) with an NADH regeneration system (Fig. 3C).

Directed evolution of TDO by error-prone PCR

The reductase TDO was chosen for random mutation by error-prone PCR to improve its catalytic activity. The improved mutants from the mutant library (over 3,000 clones) were screened by assaying the consumption of NADH using 96-well plates. Nine mutants were obtained with the improved activity toward NADH compared to the wild-type TDO (Fig. S3), and the purified mutants of MT2 and MT9 showed a 1.8- and 2.25-fold increase of relative activity compared with that of wild-type (WT), respectively (Fig. 4A). The MT2 (L127F/S139C/L316Q/V422A/D461G) and MT9 (G199S/G205R/S223N/N396S/P441S) mutants improved the activity toward NADH. MT2 and MT9 also showed the higher activity, with an affinity of 56.63 and 48.13 μM and catalytic efficiencies of 1.19 and 1.62 s^{-1} μM^{-1}, respectively (Table 1 and Fig. 4B). The yields of 9OHAD by MT2 and MT9 were significantly improved to 69.3 and 74.8%, respectively (Fig. 4C), which indicated that the efficiency of electron transfer in MT2 and MT9 had been strengthened compared with WT. The structure of TDO showed that G205, S139, L127, G199, and S223 were located in the NADH binding domain. L316 and N396 were located at the FAD-binding domain. P441 and D461 were located at [2Fe-2S] cluster domain of TDO-F (Fig. 4D)

Structural analysis of iron–sulfur clusters in KshB and TDO

Both the KshB and TDO reductases contain FAD and NADH binding domains in the N-terminal region and iron–sulfur clusters at the C terminus (Figs. 5A and B). The iron–sulfur clusters are crucial in the mediating electron transfer processes in forms of [2Fe-2S], [3Fe-4S], and [4Fe-4S] clusters [22, 23]. TDO

belongs to Rieske [2Fe-2S] ($Fe_2S_2Cys_2His_2$), and the cluster was composed of H44, H64, C42, and C61 (Fig. 5A), whereas each iron atom was coordinated by one sulfur from two Cys thiolates and two His residues. Meanwhile, KshB is a plant-type one ($Fe_2S_2Cys_4$) and is composed of C306, C310, C314, and C344. The iron atoms are coordinated by four Cys residues (Fig. 5B). The reaction depends on an electron transport chain that transfers electrons from the NADH to FAD and then to the [2Fe-2S] cluster of KshB (Fig. 5B). The electrons continue to be transferred to [2Fe-2S] cluster of the terminal oxygenase KshA for hydroxylation of steroidal substrates. When removing both [2Fe-2S] cluster domains in KshB and TDO reductases, there was no activity detected toward AD (Figs. 5C and D), which indicates that the [2Fe-2S] cluster domain plays an important role of in the electron transfer chain. Interestingly, the addition of the Rieske [2Fe-2S] cluster from TDO-F to the N terminus of KshB and TDO showed remarkably improved yields (TDO-F+KshB: 56.1% and TDO-F+TDO: 74.5%) toward AD. Meanwhile, the addition of the plant-type [2Fe-2S] cluster from KshB (pFeS) showed yields (pFeS+KshB: 47.3% and pFeS+TDO: 65.6%) compared with that of wild-type of KshB (42%) and TDO (54.8%), respectively (Fig. 4D). Therefore, the Rieske [2Fe-2S] cluster used in this electron transfer system showed a higher bioconversion yield of 9OHAD than that of the plant-type cluster. This also implied that the Rieske [2Fe-2S] cluster made the electron transfer more efficient in this KSH system.

Optimizing reaction conditions to improve 9OHAD yield

To increase the 9OHAD yield, the reaction conditions (organic co-solvents, CDs, biomass, and concentrations of AD) were further optimized by whole-cell biotransformation using the BLKA-KB-F strain with NADH regeneration; various organic co-solvents including methanol, ethanol, isopropyl alcohol, acetone, DMSO, and DMF and the surfactants Tween 80 and Triton X-100 were used to improve AD solubility in the aqueous phase in the range of 1-100 μM. When 3 vol% methanol and DMSO were used as an optimal co-solvent, the higher yields of 9OHAD were obtained with 54% and 56%, respectively. However, the 9OHAD yield decreased to 48% and 39.5% when 5 vol% co-solvents were used (Fig. 6A). This may be due to the cell membrane swelling and denaturation of membrane-associated proteins caused by high organic solvent concentrations [20].

CDs have been used widely to improve steroid solubility in aqueous media due to their hydrophilic outer surfaces and hydrophobic cavities [24, 25]. The effect of different molar ratios of CDs and AD was investigated, and the highest yields of 9OHAD were obtained when Me-β-CD (67%) and γ-CD (65.5%) were used (Fig. 6B). Therefore, Me-β-CD was used for further research due to its lower cost compared with γ-CD [26].

To investigate the influence of biomass on the yield of 9OHAD, various concentrations of recombinant cells were used, from 10 to 100 g/L. As shown in Fig. 6C, the yield of 9OHAD rose with increasing of the concentrations of cells. After 6 h, the highest yield of 9OHAD was obtained from AD at 50 g/L wet cells. The 9OHAD yields were not increased by the addition of higher concentrations of biomass. This was also consistent with previous reports for biotransformation of cortisone to 11β-hydrocortisone using *E. coli* as a whole-cell biocatalyst [20], and phytosterols to 5α-AD by recombinant *M. neoaurum* cells [27]. This may

have been to the insufficient oxygen input and distribution in reactions with high cell mass, and oxygen availability playing a crucial role in monooxygenase-catalyzed reactions [28].

Excessive substrates are difficult to dissolve even using Me-β-CD. The influence of the concentrations of AD for the bioconversion of 9OHAD was also investigated. The yield of 9OHAD decreased gradually with a concentration increases of AD, and a maximum yield was achieved at 89% when 1 g/L AD was used. However, the maximum production of 9OHAD (4.11 g/L) was obtained when 5 g/L AD was used compared with that when 1 g/L AD (0.94 g/L) and 3 g/L AD (2.72 g/L) were used. Furthermore, when 7 and 9 g/L AD were used, the yields of 9OHAD were reduced to 46% (3.40 g/L) and 32.9% (3.12 g/L), respectively (Fig. 6D). Therefore, 5 g/L AD was used for further study.

Bioconversion of AD to produce 9OHAD

To improve the yield of 9OHAD, different recombinant *E. coli* BL21(DE3) cells harboring plasmids carrying the genes for FDH, KshA, and KshB or TDO were constructed (Table 1). For efficient co-expression of all three proteins in one host and two vectors (pET28a and pETDuet-1/pCold I) were used, resulting in an engineered strain carrying the genes for the oxygenase KshA for hydroxylation, ferredoxin reductases for electron transfer, and FDH for NADH regeneration. We constructed 10 recombinant strains as described in Table 1. The resting cells of BLKA-T-F showed the high yields of 9OHAD (84.5%), followed by BLKA-KB-F cells at 72.1% (Fig. S4). It indicated that co-expression of the reductase TDO/KshB and FDH genes in pETDuet-1 played an important role in the NADH regeneration system to produce 9OHAD. The pETDuet-1 plasmid with two promoters and multiple cloning sites, is often successfully used for the construction of whole-cell biocatalysts systems with cofactor regeneration systems [29]. The introduction of reductase TDO/KshB and FDH genes in pETDuet-1 seemed to improve the efficiency of the electron transfer chain. Notably, co-expression of oxygenase KshA and reductase TDO/KshB genes in pETDuet-1 also showed the considerable yields of 9OHAD at 67.5 and 61.3%, respectively. It is obvious that the expression of the FDH gene in independently may slightly affect the efficiency of NADH regeneration. The resting cells of BLKA-T and BLKA-KB without NADH regeneration only had the yields of 9OHAD at 59.5 and 45.6%, respectively. However, there was little product of 9OHAD detected in the cells BLKA-KBF and BLKA-TF, where the reductase of KshB or TDO was linked with FDH in pCold I. This may have been due to an inappropriate linker peptide leading to the incorrect folding of KshB/TDO and FDH [30]. The overexpression of the reductase KshB or TDO with FDH genes using one promoter may increase the cellular stress during cell growth, even as the cold shock gene of *csp*A was designed for use with pCold I.

The TDO mutant (MT9) gene was inserted into pETDuet-1 instead of TDO wild type and then transformed into BL21(DE3) together with KshA and the FDH gene. The resting cells of BLKA-T-F, BLKA-KB-F, BLKA-TM-F, and BLKA-RTM-F were then used to convert AD to 9OHAD. Comparing with the resting cells of BLKA-T-F and BLKA-KB-F with the space-time yields of 9OHAD at 0.72 g/(L·h) and 0.65 g/(L·h), the resting cells of the strain BLKA-TM-F further increased the yield of 9OHAD. It completely converted 5 g/L AD to 5.19 g/L 9OHAD within 6 h (Fig. 7 and Table 3), with a space-time yield of 0.87 g/(L·h). The construction of a modified TDO mutant with a Rieske [2Fe-2S] cluster at the N terminus (BLKA-RTM-F) showed a higher

production and space-time yield of 5.24 g/L and 1.05 g/(L·h) of 9OHAD, respectively. An efficient electron transfer system has improved the yields of 9OHAD in these whole-cell catalysts.

In comparison, the biosynthesis of 9OHAD are extensively studied by the engineered *Mycobacterium* using phytosterol as substrate. Xiong *et al.* constructed a 9-OHAD-producing strain with productivity of 10.27 g/L (0.071 g/(L·h)) from 20 g/L phytosterol by deletion of a sigma factor D (*sigD*) and overexpression of a cholesterol oxidase ChoM2 [31]. They further achieved the productivity of 0.114 g/(L·h) by deleting *kasB* gene encoding a β-ketoacyl-acyl carrier protein synthase in *M. neoaurum* ATCC 25795 strain to improve the cell permeability [32]. Yao *et al.* demonstrated a stable accumulation of 9-OHAD with productivity of 7.33 g/L (0.051 g/(L·h)) from 15 g/L phytosterol by multiple deletions of three KstD genes and overexpression of the KshA gene in *M. neoaurum* ATCC 25795 strain [11]. Furthermore, they improved the production of 9OHAD to 11.7 g/L (0.098 g/(L·h)) from 20 g/L phytosterol by overexpression of a mutant $KshA1_N$ in engineered *M. neoaurum* ATCC 25795 strain [8]. The 9OHAD production and space-time yield reached 19.64 g/L and 0.82 g/(L·h) from 20 g/L AD using whole cells of modified *R. erythropolis* RG1-UV29 strains without KstD activity [33]. Gao *et al*. reported that the 9OHAD production and space-time yield could reach 36.4 g/L and 0.379 g/(L·h) from 70 g/L phytosterol with resting cells of *M. neoaurum* NwIB-yV in a 5-L bioreactor, respectively [12]. However, the production of 9OHAD could only reach 0.63 g/L (0.01 g/(L·h)) from 1 g/L AD using whole cells of recombinant *E. coli* [4], and 7.23 g/L (0.45 g/(L·h)) from 8 g/L AD using whole-cells recombinant *B. subtilis*, respectively [34]. Thus, the constructed BLKA-RTM-F was a great 9OHAD producer with high production of 5.24 g/L and space-time yield of 1.05 g/(L·h), a considerable yield of 99.3% of theoretical without by-products.

Conclusions

We constructed a green, convenient, and efficient synthetic pathway for 9OHAD production. An NADH regeneration system by expressing FDH was introduced, and the protein engineering technology was used to screen and improve the catalytic activity of reductases because these are the rate-limiting step in the bioconversion of AD. Increasing the strength of electron transfer efficiency in the KSH hydroxylation reaction by the addition of a Rieske [2Fe-2S] cluster was another strategy to increase the yield of 9OHAD. Finally, a 99.3% molar yield (5.24 g/L) of 9OHAD was obtained without by-products using the resting cells of BLKA-RMT-F, which contained the cofactor recycling system and a modified TDO mutant with a Rieske [2Fe-2S] cluster at the N terminus after optimizing the biotransformation conditions. This research provides new insight into the use of NADH regeneration systems and higher efficient bioconversion of steroidal substrates by protein engineering.

Materials And Methods

General information and materials

The details of bacterial strains, plasmids, and chemicals are listed in the Electronic Supplementary Information (ESI), and all reagents were purchased from commercial suppliers, unless otherwise stated.

All primers and plasmids used in this study are listed in Table S1.

Plasmids construction, expression, and purification of enzymes

E. coli strains BL21 (DE3) and JM109, and the vectors pCold I, pET28a, and pETDuet-1, were purchased from Novagen (Madison, WI, USA) and stored in the laboratory. The strain JM109 was used as a host organism for cloning, and BL21 (DE3) was implemented for expression. The detailed strains and plasmids used in this study are listed in Tables 1 and S1. The methods to construct vectors and express and purify the reductases and KshA are described in the ESI.

Activity assays

FDH activity was monitored by following UV absorption at a wavelength of 340 nm using a multi-mode plate reader (SpectraMax i3x, Molecular Devices, Silicon Valley, CA, USA). The reaction mixture contained 1.75 mM sodium formate, 500 μM NAD^+, and 0.25 μM FDH in PBS buffer (pH 7.4). The activities of reductases were carried out in PBS buffer (pH 7.4) with NADH as a substrate and monitored by the UV absorption at a wavelength of 340 nm. The concentrations of NADH were quantified by continuously recording the changing of the absorbance at 340 nm (ε = 6.22 mM^{-1} cm^{-1}) [35]. One unit was defined as the amount of the enzyme that catalyzed the formation of 1 μmol NAD^+ (reductases) or NADH (FDH) per min at 35 °C and pH 7.4. All of the assays were performed in triplicate independently, and the data are shown as the mean ± SD.

The steady-state kinetic parameters for FDH were determined with NAD^+ (10-300 μM) as the substrates at a formate concentration of 200 mM at 35 °C and 50 mM PBS (pH 7.4) containing 0.5 μM purified enzyme. The steady-state kinetic parameters of reductases were determined with NADH (10-300 μM) as a substrate, and data were analyzed by fitting to the Michaelis-Menten equation using Graphpad Prism 7.0 software (Graphpad Software, La Jolla, CA) to obtain the kinetic parameters k_{cat} and K_m. All of the assays were performed in triplicate independently, and the data are shown as the mean ± SD.

Confirmation of products using HPLC

The reaction mixture (1 mL) contained 50 mM potassium phosphate buffer (pH 7.4), 500 μM NADH, 5 μM KshB, 2.5 μM KshA, and 500 μM AD dissolved in 2% methanol at 35 °C [4]. One unit of enzyme activity was defined as the amount of enzyme required to consume 1 μmol of AD per min under the standard assay conditions.

Denatured protein was removed by centrifugation at 8,000 × *g* for 5 min, and the reaction product 9OHAD was extracted with 0.5 mL ethyl acetate twice and dried under nitrogen flow. The product was dissolved in 20 μL methanol and analyzed on an Agilent 1260 Infinity HPLC instrument (Agilent Technologies, Santa Clara, CA, USA) equipped with a Diamensil C18 column (4.6 × 250 nm, id 5 μm; Dikma Technologies, Beijing, China). The column was eluted at 35 °C with 80% methanol in water at a flow rate of 0.8 mL/min, and the product was detected at 254 nm.

Random mutagenesis of TDO reductase

A TDO mutant library was generated using the GeneMorph II Random Mutagenesis Kit (Agilent Technologies, Texas, TX, USA) as previously reported [36]. The mutagenic primers TDOMT_F and TDOMT_R are listed in Table S1. The TDO mutant genes were inserted into the pCold I vector linearized with *Nde*I using the NEBuilder high-fidelity DNA assembly cloning kit (NEB, Ipswich, MA, USA). Plasmids containing the TDO mutant were then transformed into *E. coli* BL21(DE3) cells by heat shock for screening the mutants with higher activity toward NADH.

The individual mutants were cultured in 96-well plates in 200 μL lysogeny broth (LB) medium containing 50 μg/mL kanamycin at 37 °C. IPTG was then added at a final concentration of 0.5 mM until the OD_{600} reached 0.6-0.8 for the protein overexpression. The cells were harvested at 4,000 × *g* for 20 min and resuspended in 200 μL potassium phosphate buffer (50 mM, pH 7.4) containing 0.5 mg/mL lysozyme, 1× BugBuster (EMD Millipore, CA, USA), 1 mM dithiothreitol (DTT), and 1 mM PMSF. After incubation at 30 °C shaking for 2 h, the cell debris were removed by centrifugation (4,000 × *g*, 20 min), and the clear supernatants were used to determine the activity of mutant enzymes.

Multienzyme cascade catalysis *in vitro*

The production of 9OHAD from AD by cell-free multienzyme catalysis was performed using a reaction mixture including 50 mM potassium phosphate buffer (pH 7.4), 500 μM AD dissolved in 2% methanol, 1.75 mM sodium formate, 500 μM NAD^+, and enzymes (5 μM reductases, 2.5 μM KshA, and 0.25 μM FDH). The yields of 9OHAD were determined using HPLC as above.

Construction of whole-cell catalysis for the transformation of AD

The constructed recombinant plasmids and strains are listed in Table 1. The whole-cell catalysis with different combinations including the plasmids of pET28a, pETDuet-1, or pCold I bearing genes encoding FDH, KshA, KshB, and TDO in *E. coli* BL21 (DE3) was used to transform AD. The detailed methods are described in the ESI.

Optimization of reaction conditions for AD transformation

The cells were harvested by centrifugation at 8,000 × *g* for 15 min and resuspended in 30 mL 50 mM potassium phosphate buffer (pH 7.4) in 250-mL shake flasks for catalyzing AD to 9OHAD. Sodium formate was added as an NADH regeneration system in the reaction mixture.

The organic co-solvents methanol, ethanol, isopropyl alcohol, acetone, DMSO, and *N, N*-Dimethylformamide (DMF) and the surfactants Tween 80 and Triton X-100 were added at various concentrations from 1.0 to 5.0% (*v*/*v*) to enhance substrate solubility. Four cyclodextrins (CDs), including β-cyclodextrin, γ-cyclodextrin, hydroxypropyl-β-cyclodextrin (HP-β-CD), and methylated-β-cyclodextrin (Me-β-CD), were also added as substrate cosolvents. Various substrates concentrations (1, 3, 5, 7, and 9 g/L) were optimized to determine yields of 9OHAD. Finally, the effect of the amount of the whole-cell biomass

(10, 20, 30, 50, 70, and 100 g/L, wet cell weight) on the yield of 9OHAD was investigated. Samples were determined and analyzed by HPLC.

Abbreviations

9OHAD 9α-hydroxy4-androstene-3,17-dione

AD 4-androstene-3,17-dione

FDH Formate dehydrogenase

DMF *N, N*-Dimethylformamide

CD cyclodextrin

HP-β-CD hydroxypropyl-β-cyclodextrin

Me-β-CD methylated-β-cyclodextrin

Declarations

Acknowledgements

Not applicable.

Authors' contributions

FL, MT, and H-MQ designed the research; ZZ, XG, and ZS performed the experiments, ZZ, XG, and CL conducted the data analysis and prepared the manuscript. FL, MT, and H-MQ helped to revise the manuscript. All authors read and approved the final manuscript.

Funding

This work was supported by National Natural Science Foundation of China (31771911).

Availability of data and material

All data generated and analyzed in this study are included in this published article.

Ethics approval and consent to participate

Not applicable.

Consent for publication

Not applicable.

Competing interests

The authors declare that they have no Competing interests.

References

1. Donova MV, Egorova OV. Microbial steroid transformations: current state and prospects. Appl Microbiol Biotechnol. 2012;94:1423–1447.
2. Donova MV. Transformation of steroids by actinobacteria: A review. Appl Biochem Microbiol. 2007;43:1-14.
3. Fernandes P, Cruz A, Angelova B, Pinheiro HM, Cabral JMS. Microbial conversion of steroid compounds: recent developments. Enzyme Microb Technol. 2003;32:688-705.
4. Petrusma M, Dijkhuizen L, van der Geize R. *Rhodococcus rhodochrous* DSM 43269 3-ketosteroid 9α-hydroxylase, a two-component iron-sulfur-containing monooxygenase with subtle steroid substrate specificity. Appl Environ Microbiol. 2009;75:5300-5307.
5. Capyk JK, D'Angelo I, Strynadka NC, Eltis LD. Characterization of 3-ketosteroid 9α-hydroxylase, a Rieske oxygenase in the cholesterol degradation pathway of *Mycobacterium tuberculosis*. J Biol Chem. 2009;284:9937-9946.
6. Petrusma M, Hessels G, Dijkhuizen L, van der Geize R. Multiplicity of 3-ketosteroid-9α-hydroxylase enzymes in *Rhodococcus rhodochrous* DSM43269 for specific degradation of different classes of steroids. J Bacteriol. 2011;193:3931-3940.
7. van der Geize R, Hessels GI, Gerwen Rv, Meijden Pvd, Dijkhuizen L. Molecular and functional characterization of kshA and kshB, encoding two components of 3-ketosteroid 9α-hydroxylase, a class IA monooxygenase, in *Rhodococcus erythropolis* strain SQ1. Mol Microbiol. 2002;45:1007-1018.
8. Liu HH, Xu LQ, Yao K, Xiong LB, Tao XY, Liu M, et al. Engineered 3-ketosteroid 9α-hydroxylases in *Mycobacterium neoaurum*: an efficient platform for production of steroid drugs. Appl Environ Microbiol. 2018;84:e02777-02717.
9. Andor A, Jekkel A, Hopwood DA, Jeanplong F, Ilkoy E, Konya A, et al. Generation of useful insertionally blocked sterol degradation pathway mutants of fast-growing mycobacteria and cloning, characterization, and expression of the terminal oxygenase of the 3-ketosteroid 9α-hydroxylase in *Mycobacterium smegmatis* mc2 155. Appl Environ Microbiol. 2006;72:6554-6559.
10. Arnell R, Johannisson R, Lindholm J, Fornstedt T, Ersson B, Ballagi A, et al. Biotechnological approach to the synthesis of 9α-hydroxylated steroids. Prep Biochem Biotechnol. 2007;37:309-321.
11. Yao K, Xu LQ, Wang FQ, Wei DZ. Characterization and engineering of 3-ketosteroid-Δ^1-dehydrogenase and 3-ketosteroid-9α-hydroxylase in *Mycobacterium neoaurum* ATCC 25795 to produce 9α-hydroxy-4-androstene-3,17-dione through the catabolism of sterols. Metab Eng. 2014;24:181-191.

12. Gao XQ, Feng JX, Wang XD, Hua Q. Enhanced steroid metabolites production by resting cell phytosterol bioconversion. Chem Biochem Eng Q. 2016;29:567-573.
13. Finnigan W, Cutlan R, Snajdrova R, Adams JP, Littlechild JA, Harmer, NJ. Engineering a seven enzyme biotransformation using mathematical modelling and characterized enzyme parts. Chemcatchem. 2019;11:3474-3489.
14. Yu S, Zhu L, Zhou C, An T, Jiang B, Mu W. Enzymatic production of D-3-phenyllactic acid by *Pediococcus pentosaceus* D-lactate dehydrogenase with NADH regeneration by *Ogataea parapolymorpha* formate dehydrogenase. Biotechnol Lett. 2014;36:627-631.
15. van der Donk WA, Zhao H. Recent developments in pyridine nucleotide regeneration. Curr Opin Biotechnol. 2003;14:421-426.
16. Wang Y, Li L, Ma C, Gao C, Tao F, X P. Engineering of cofactor regeneration enhances (2*S*, 3*S*)-2,3-butanediol production from diacetyl. Sci Rep. 2013;3:2643.
17. Jaroensuk J, Intasian P, Kiattisewee C, Munkajohnpon P, Chunthaboon P, Buttranon S, et al. Addition of formate dehydrogenase increases the production of renewable alkane from an engineered metabolic pathway. J Biol Chem. 2019;294:11536-11548.
18. Samuel N, Bao T, Zhang X, Yang T, Xu M, Li X, et al. Optimized whole cell biocatalyst from acetoin to 2,3-butanediol through coexpression of acetoin reductase with NADH regeneration systems in engineered *Bacillus subtilis*. J Chem Technol Biotechnol. 2017;92:2477-2487.
19. Janocha S, Bernhardt R. Design and characterization of an efficient CYP105A1-based whole-cell biocatalyst for the conversion of resin acid diterpenoids in permeabilized *Escherichia coli*. Appl Microbiol Biotechnol. 2013;97:7639–7649.
20. Shao M, Zhang X, Rao Z, Xu M, Yang T, Li H, et al. Efficient testosterone production by engineered *Pichia pastoris* co-expressing human 17β-hydroxysteroid dehydrogenase type 3 and *Saccharomyces cerevisiae* glucose 6-phosphate dehydrogenase with NADPH regeneration. Green Chem. 2016;18:1774-1784.
21. Friemann R, Lee K, Brown EN, Gibson DT, Eklund H, Ramaswamy, S. Structures of the multicomponent Rieske non-heme iron toluene 2,3-dioxygenase enzyme system. Acta Crystallogr D: Biol Crystallogr. 2009;65:24-33.
22. Dizicheh ZB, Halloran N, Asma W, Ghirlanda G. De novo design of iron-sulfur proteins. Methods Enzymol. 2017;595:33-53.
23. Liu J, Chakraborty S, Hosseinzadeh P, Yu Y, Tian S, Petrik I, et al. Metalloproteins containing cytochrome, iron-sulfur, or copper redox centers. Chem. Rev. 2014;114:4366-4469.
24. Zhang L, Wang M, Shen Y, Ma Y, Luo J. Improvement of steroid biotransformation with hydroxypropyl-β-cyclodextrin induced complexation. Appl Biochem Biotechnol. 2009;159:642-654.
25. Manosroi A, Saowakhon S, Manosroi J. Enhancement of androstadienedione production from progesterone by biotransformation using the hydroxypropyl-β-cyclodextrin complexation technique. J Steroid Biochem Mol Biol. 2008;108:132-136.

26. Zhou X, Zhang Y, Shen Y, Zhang X, Xu S, Shang Z, et al. Efficient production of androstenedione by repeated batch fermentation in waste cooking oil media through regulating NAD(+)/NADH ratio and strengthening cell vitality of *Mycobacterium neoaurum*. Bioresour Technol. 2019;279:209-217.
27. Zhao Y, Shen Y, Ma S, Luo J, Ouyang W, Zhou H, et al. Production of 5α-androstene-3,17-dione from phytosterols by co-expression of 5α-reductase and glucose-6-phosphate dehydrogenase in engineered *Mycobacterium neoaurum*. Green Chem. 2019;21:1809-1815.
28. Bracco P, Janssen DB, Schallmey A. Selective steroid oxyfunctionalisation by CYP154C5, a bacterial cytochrome P450. Microb Cell Fact. 2013;12:95.
29. Liu S, Zhang X, Liu F, Xu M, Yang T, Long M, et al. Designing of a cofactor self-sufficient whole-cell biocatalyst system for production of 1,2-amino alcohols from epoxides. ACS Synth Biol. 2019;8:734-743.
30. Li B, Li Y, Bai D, Zhang X, Yang H, Wang J, et al. Whole-cell biotransformation systems for reduction of prochiral carbonyl compounds to chiral alcohol in *Escherichia coli*. Sci Rep. 2014;4:6750.
31. Xiong LB, Liu HH, Xu LQ, Wei DZ, Wang FQ. Role identification and application of SigD in the transformation of soybean phytosterol to 9α-hydroxy-4-androstene-3,17-dione in *Mycobacterium neoaurum*. J Agric Food Chem. 2017;65:626-631.
32. Xiong LB, Liu HH, Zhao M, Liu YJ, Song L, Xie ZY, et al. Enhancing the bioconversion of phytosterols to steroidal intermediates by the deficiency of *kas*B in the cell wall synthesis of *Mycobacterium neoaurum*. Microb Cell Fact. 2020;19:1-11.
33. van der Geize R, Hessels GI, van Gerwen R, van der Meijden P, Dijkhuizen L. Unmarked gene deletion mutagenesis of *kst*D, encoding 3-ketosteroid Δ1-dehydrogenase, in *Rhodococcus erythropolis* SQ1 using *sac*B as counter-selectable marker. FEMS Microbiol Lett. 2001;205:197-202.
34. Zhang X, Rao Z, Zhang L, Xu M, Yang T. Efficient 9α-hydroxy-4-androstene-3,17-dione production by engineered *Bacillus subtilis* co-expressing *Mycobacterium neoaurum* 3-ketosteroid 9α-hydroxylase and *B. subtilis* glucose 1-dehydrogenase with NADH regeneration. Springerplus. 2016;5:1207.
35. Zhang Y, Huang Z, Du C, Li Y, Cao Z. Introduction of an NADH regeneration system into *Klebsiella oxytoca* leads to an enhanced oxidative and reductive metabolism of glycerol. Metab Eng. 2009;11:101-106.
36. Sun D, Gao D, Liu X, Zhu M, Li C, Chen Y, et al. Redesign and engineering of a dioxygenase targeting biocatalytic synthesis of 5-hydroxyl leucine. Catal Sci Technol. 2019;9:1825-1834.

Tables

Table 1 Bacterial strains used in this study

Strains	Description	Source
E. coli JM109	Host of plasmid for cloning	Lab stock
E. coli BL21	Host of plasmid for expression	Lab stock
BLKA-KB	pET28a carries KshA, pCold carries KshB	This study
BLKA-T	pET28a carries KshA, pCold carries TDO	This study
BLKA-KB-F	pET28a carries KshA, pETDuet carries KshB and FDH	This study
BLKA-T-F	pET28a carries KshA, pETDuet carries TDO and FDH	This study
BLKA-TM-F	pET28a carries KshA, pETDuet carries TDOMT9 and FDH	This study
BLKA-RTM-F	pET28a carries KshA, pETDuet carries TDO-F-TDOMT9 and FDH	This study
BLKA-KBF	pET28a carries KshA, pCold carries KshB and FDH	This study
BLKA-TF	pET28a carries KshA, pCold carries TDO and FDH	This study
BLKB-KA-F	pET28a carries FDH, pETDuet carries KshB and KshA	This study
BLT-KA-F	pET28a carries FDH, pETDuet carries TDO and KshA	This study

Table 2 Kinetic parameters of reductases toward NADH

Reductase	K_m (μmol)	k_{cat} (s^{-1})	k_{cat}/K_m (s^{-1} μM^{-1})	Yield (%)
DMR1	55.72 ± 2.84	20.62 ± 0.59	0.37	45.2 ± 1.36
DMR2	103 ± 4.56	21.84 ± 0.76	0.21	29.9 ± 1.25
DMR3	182.1 ± 8.85	19.44 ± 0.79	0.11	26.5 ± 0.75
TDO	65.37 ± 2.71	28.21 ± 0.91	0.43	54.8 ± 1.74
KshB	70.85 ± 4.08	23.88 ± 1.06	0.34	42.0 ± 1.29
MT2	56.63 ± 2.72	67.5 ± 2.75	1.19	69.3 ± 2.35
MT9	48.13± 1.78	77.8 ± 1.89	1.62	74.8 ± 3.06

Table 3 Comparison of 9OHAD production using resting cells containing different plasmids.

Strains	9OHAD (g/L)	Conversion durations (h)	Space-time yield g/(L·h)
BLKA-RTM-F	5.24 ± 0.15	5	1.05
BLKA-TM-F	5.19 ± 0.08	6	0.87
BLKA-T-F	5.02 ± 0.09	7	0.72
BLKA-KB-F	4.54 ± 0.13	7	0.65

Additional File

Table S1 Primers and plasmids used in this study.

Fig. S1 The Michaelis-Menten plots of FDH toward NAD^+.

Fig. S2 The Michaelis-Menten plots of reductases toward NADH.

Fig. S3 The relative activity of TDO mutants by error-prone PCR.

Fig. S4 The yields of 9OHAD using different strains containing different plasmids.

Fig. S5 Confirmation of the enzymatic conversion of AD to 9OHAD using HPLC.

Figures

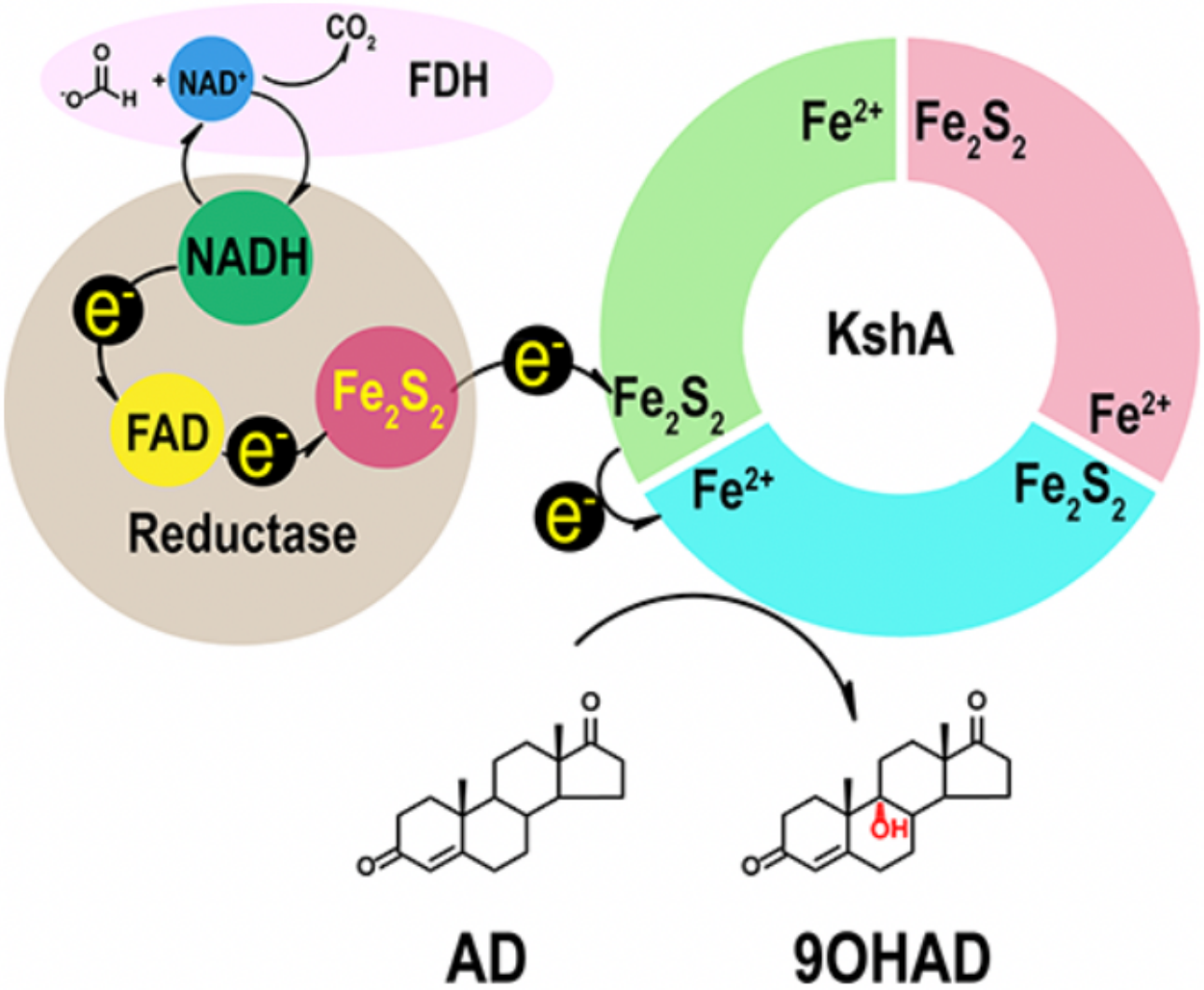

Figure 1

Schematic representation of the whole-cell system designed for AD hydroxylases. FDH: formate dehydrogenase; Reductase: ferredoxin reductase for electron transfer; KshA: the oxygenase component of 3-ketosteroid 9-hydroxylase. Formate was used as a substrate for the regeneration of NADH.

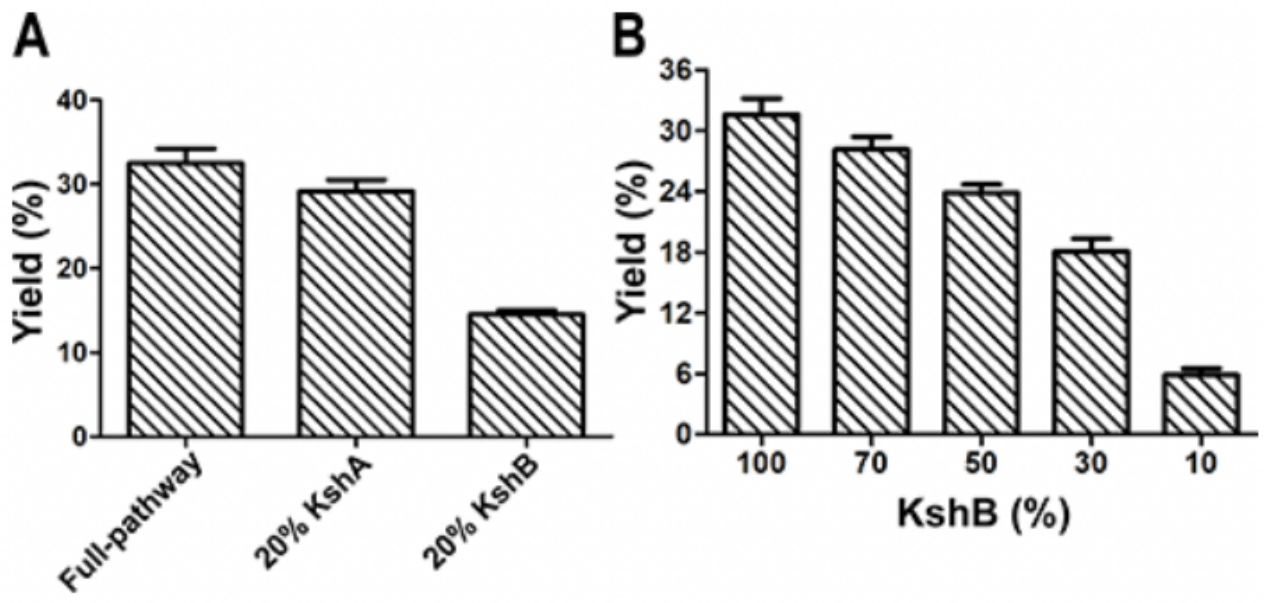

Figure 2

Analysis of the rate-limiting step in the conversion of AD to 9OHAD. (A) 100% KshAB was used as a control, and the concentrations of KshA and KshB were reduced to 20%. (B) The yields of 9OHAD with 100% KshA and reduced concentrations of KshB. Data are shown as the mean ± SD of three independent experiments.

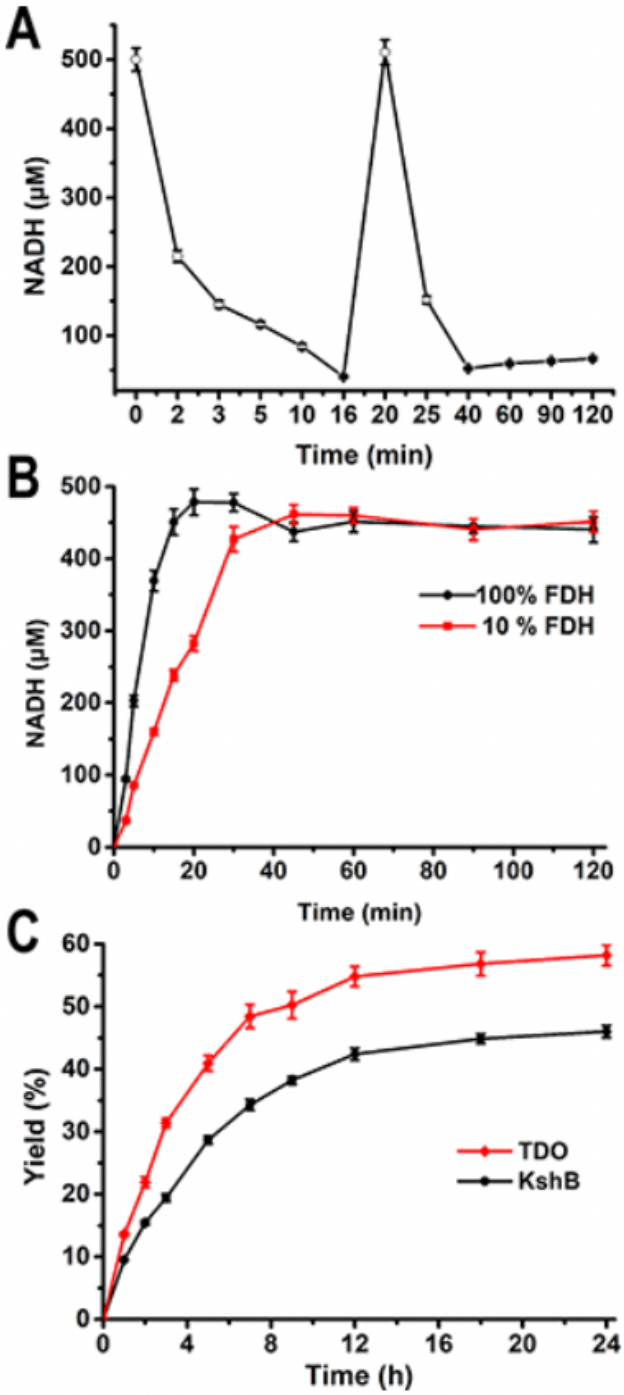

Figure 3

(A) Time-course of the consumption of NADH at 340 nm, 500 μM NADH was added to the reaction system at the 0 and 20 min. (B) Time-course of NADH consumption at 340 nm when adding 10 and 100% FDH to the reaction system. (C) Time-course of the yield of 9OHAD using the reductase KshB (black line) and TDO (red line) when adding FDH to the reaction system. Data are shown as the mean ± SD from three independent experiments.

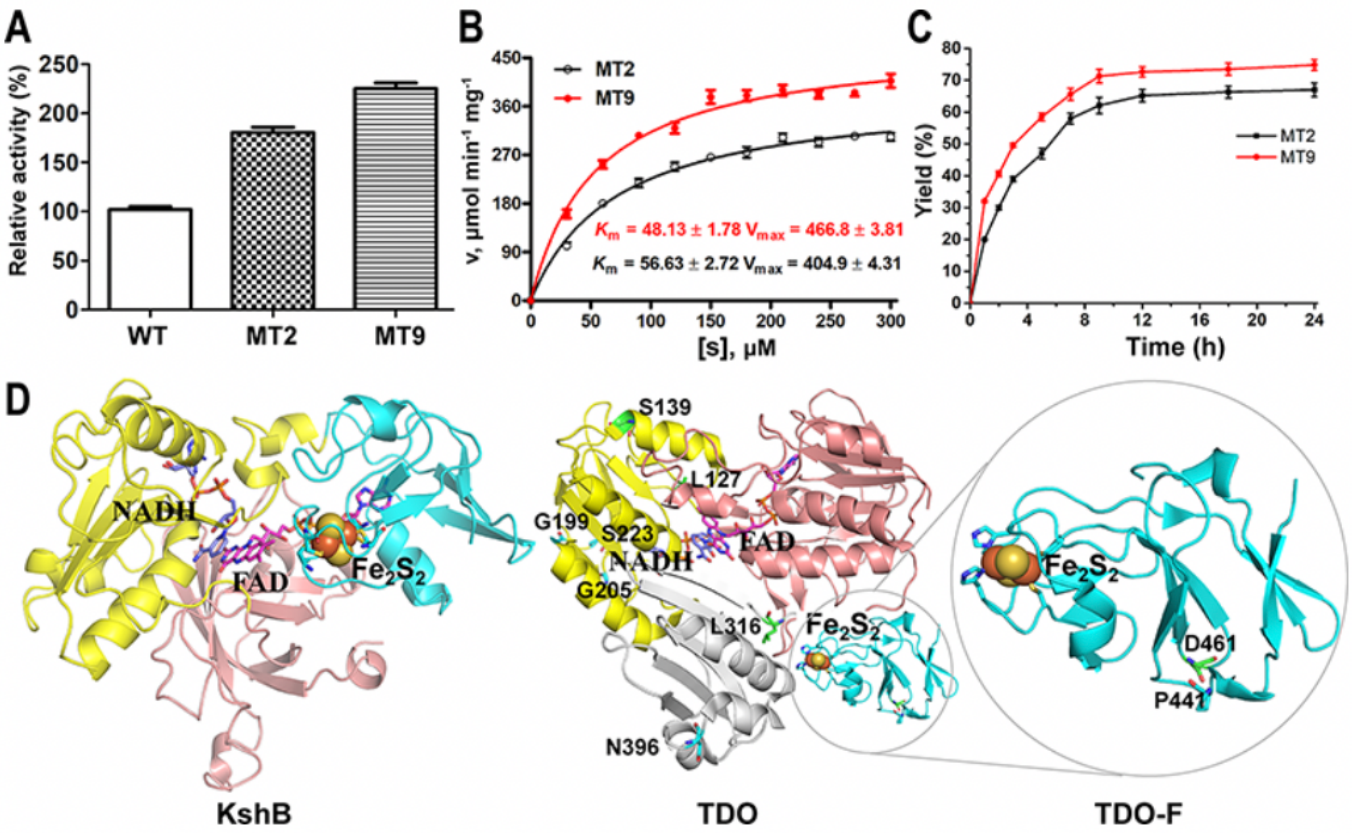

Figure 4

(A) The relative activity of purified TDO mutants toward NADH. (B) Michaelis-Menten plots of TDO mutants toward NADH. (C) Time-course of the yields of 9OHAD using TDO mutants. Data are shown as the mean ± SD from three independent experiments. (D) Overall structures of KshB and TDO in complex with FAD and NADH, iron–sulfur cluster, the FAD-binding domain, NADH-binding domain, and C-terminal domain were colored pink or red, yellow, and gray, respectively.

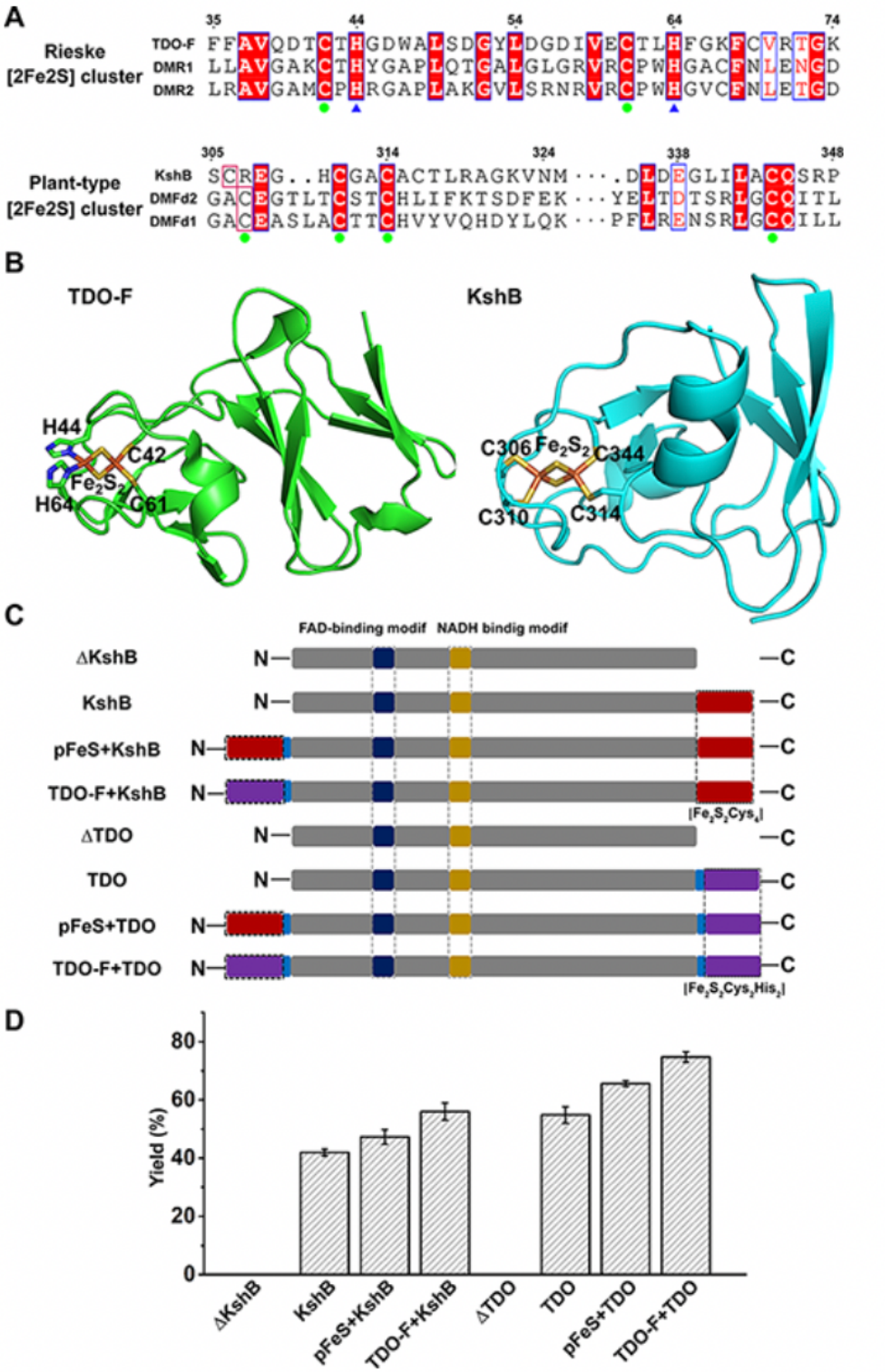

Figure 5

(A) Multiple sequence alignment of amino acids in the iron–sulfur cluster. The residues binding to the cluster are marked as green circles, and the two conserved His residues are marked as blue triangles. (B) Overall structures of the [2Fe-2S] cluster of TDO-F and KshB. (C) Schematic representation for construction of KshB and TDO with and without the [2Fe-2S] cluster. (D) The yields of 9OHAD by various modified KshB and TDO. Data are shown as the mean ± SD from three independent experiments.

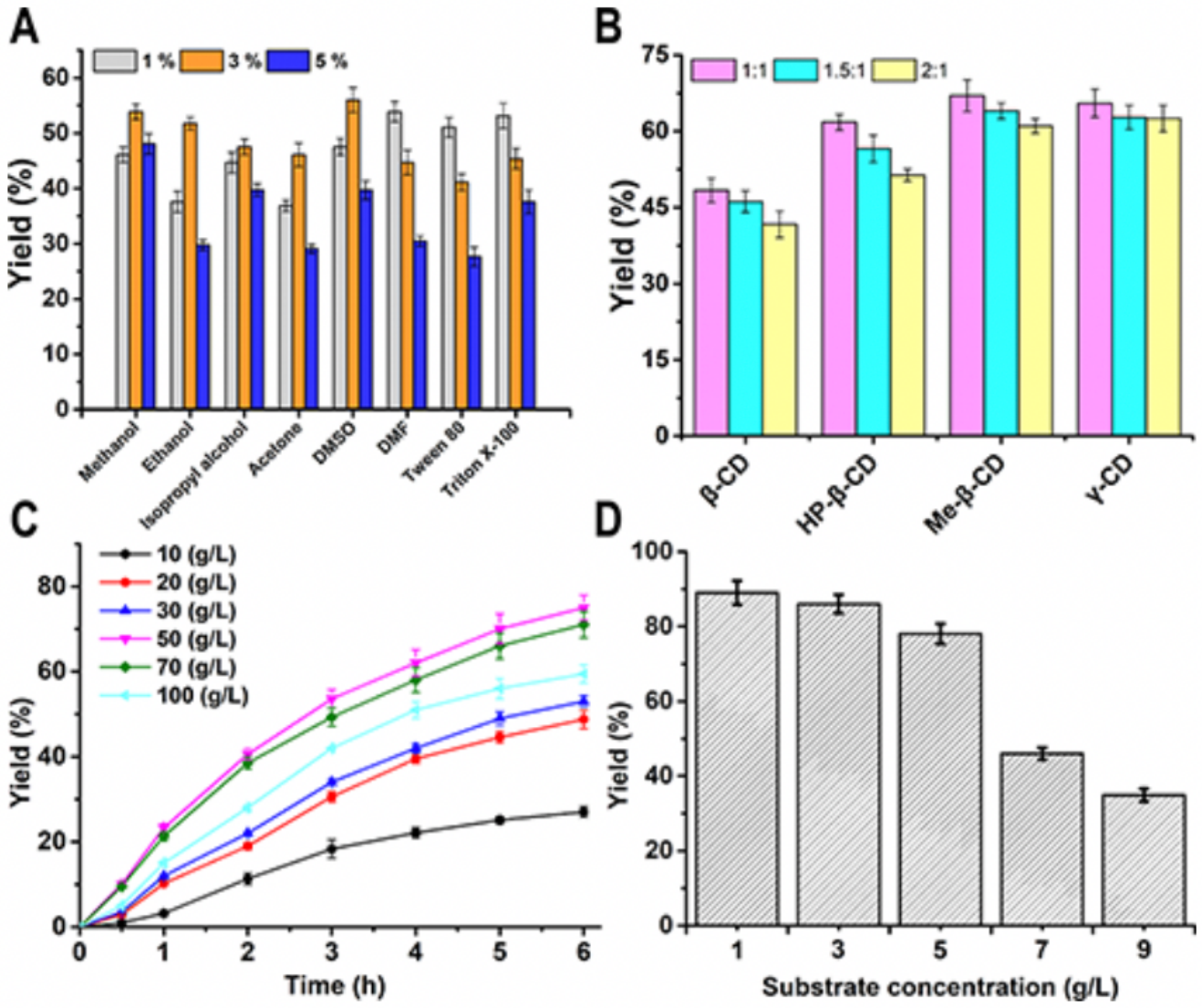

Figure 6

Effects of different co-solvents at various concentrations (1, 3, and 5 vol%, A) and molar ratios of β-CD, HP-β-CD, Me-β-CD, and γ-CD:AD (B). The yield of 9OHAD in resting cells. Effects of different biomasses (C) and substrate concentrations (D) on the yields of 9-OHAD in resting cells. Data are shown as the mean ± SD from three independent experiments.

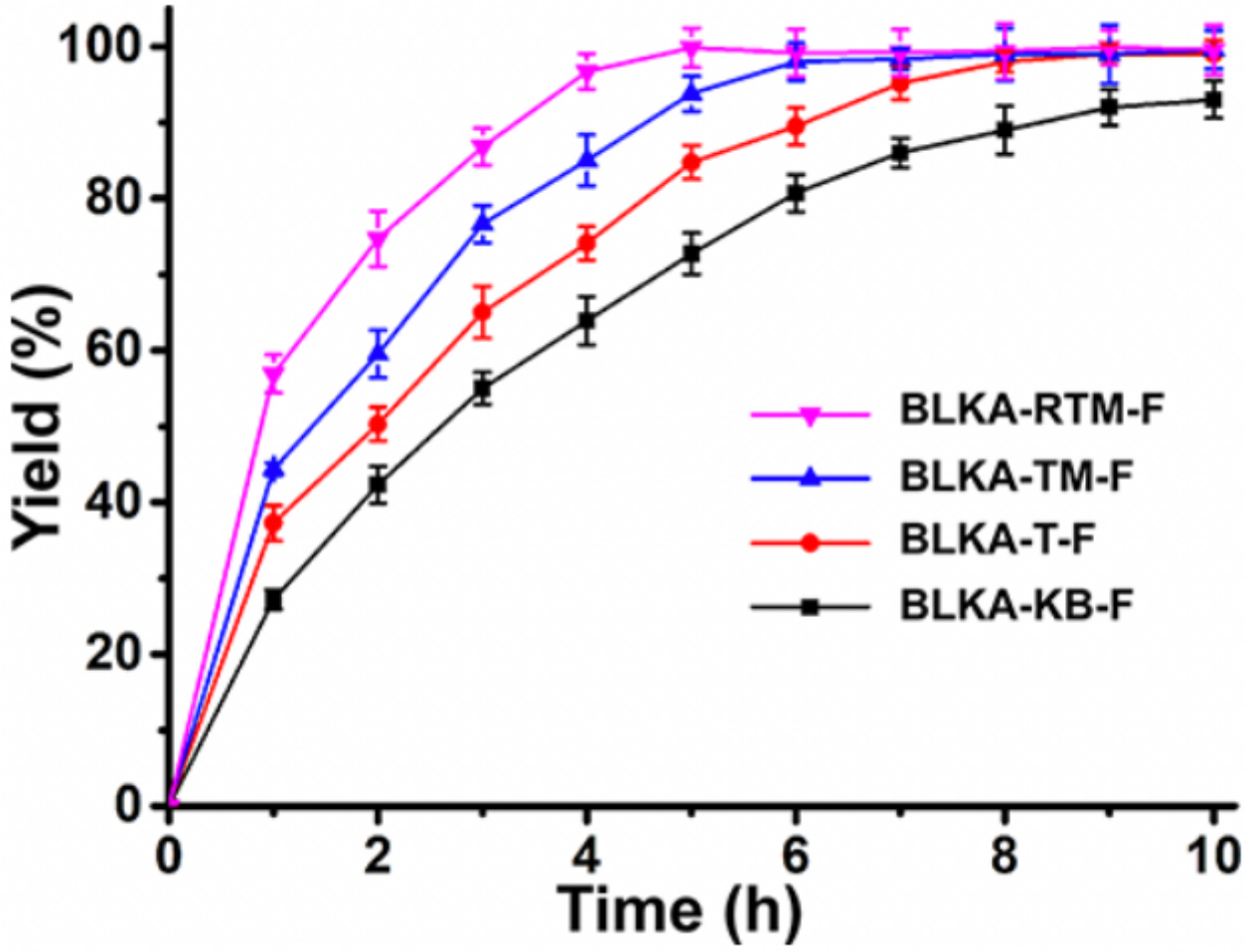

Figure 7

Time-course of the yields of 9OHAD using selected resting cells. Data are shown as the mean ± SD from three independent experiments.

Supplementary Files

This is a list of supplementary files associated with this preprint. Click to download.

- ZhuReductasesupplementarymaterialBBV1.docx